IL13 and periostin in active fibrogenic areas of the extrahepatic bile ducts in biliary atresia patients

Yuki Sengoku
Kyoto Prefectural University of Medicine
Mayumi Higashi (higashim@koto.kpu-m.ac.jp)
Kyoto Prefectural University of Medicine
Kazuya Nagayabu
Kyoto Prefectural University of Medicine
Shohei Takayama
Kyoto Prefectural University of Medicine
Shigehisa Fumino
Kyoto Prefectural University of Medicine
Shigeyoshi Aoi
Kyoto Prefectural University of Medicine
Taizo Furukawa
Kyoto Prefectural University of Medicine
Tatsuro Tajiri
Kyoto Prefectural University of Medicine

Research Article

Keywords: Biliary atresia, IL13, Periostin, Inflammation, Fibrogenesis

Posted Date: September 12th, 2022

DOI: https://doi.org/10.21203/rs.3.rs-2041441/v1

Abstract

Background: The leading pathology of biliary atresia (BA) is inflammatory and fibrous obstruction of extrahepatic bile duct, butthe pathogenesis remains unclear.IL13 is a cytokine associated with allergies and inflammatory fibrosis, and periostin induces fibrogenesis by stimulation with IL13. We analyzed the involvement of IL13 and periostin in inflammatory fibrosis in the extrahepatic bile duct of BA patients.

Materials and Methods: Surgically resected tissues from the hepatic hilar area of BA patients were immunostained with CD45, α-SMA, IL13 and periostin and statistically analyzed. Fibroblasts from the resected tissue were cultured with recombinant IL13, and periostin production was analyzed by quantitative polymerase chain reaction and Western blotting.

Results: IL13 was stained in 93% of large and micro bile ducts, and 92.1% matched with the CD45 location ($p=0.006$) around the large bile ducts. Periostin staining correlated with the localization of IL13 and αSMA ($p<0.001$) around the large bile ducts. Periostin mRNA and protein were up regulated by IL13 stimulation in cultured fibroblasts.

Conclusion: IL13 was associated with induced periostin expression by fibroblasts, playing a vital role in the pathogenesis of fibrogenesis around the extrahepatic bile duct in BA.

Introduction

Biliary atresia (BA) is a progressive cholestatic hepatopathy in infants with the pathology of inflammatory and fibrous obstruction of the extrahepatic bile ducts by an unknown etiology. If untreated, the liver develops fatal cirrhosis, and even after primary surgery, about half of patients need liver transplantation because of the progression of cirrhosis.

The standard primary surgery for BA is Kasai portoenterostomy (KPE), wherein the remnants of obstructed extrahepatic bile ducts are resected and replaced by intestine. According to histological analyses, resected tissues from the hilar area of the liver show active inflammatory fibrosis around the remnant of bile ducts, including infiltration of inflammatory cells, such as neutrophils, eosinophils and macrophages. A histological examination of the remnant is crucial for clarifying the pathogenesis, and many histological studies for BA have reported correlations between the histological features and clinical prognoses [1–8]. However, few reports have focused on the immune responses that precede fibrosis, especially around the extrahepatic bile ducts in BA.

IL13 is a type 2 immune response cytokine that causes fibrosis at the site of inflammation in various allergic diseases and inflammatory gastrointestinal diseases [9]. The type 2 immune response plays roles in tissue repairs and homeostasis. However, its chronic activity and overreaction can cause tissue damage or fibrosis [10]. IL13 is secreted from Helper T2 cells or other innate immunity cells in response to epithelial injury and promotes mucus secretion by inducing the proliferation of glandular epithelium. IL13 also participates in the activation of fibroblasts and progression of tissue fibrosis [11]. Although some

studies have demonstrated the involvement of abnormal immunological activities in BA, most were type 1 immune responses [12, 13]. Regarding IL13, few reports have suggested its contribution to BA progression, except for its presence in fibrotic liver or elevated serum levels [14, 15]. Only the involvement of IL13 in the pathogenesis of extrahepatic bile duct has been reported, and even then, only in rhesus rotavirus type A (RRV) BA model mice [16, 17], not human BA.

As another factor related to fibrosis, periostin is a cell adhesion molecule secreted from fibroblasts by IL13 stimulation. It causes fibrogenesis by binding to extracellular matrix, such as type 1 collagen. As a matricellular protein, periostin promotes cell migration and activation of inflammatory cells by binding integrin molecules, eventually causing chronicity and exacerbation of inflammation [18]. Periostin is highly expressed in allergic diseases or inflammatory fibrosis, such as asthma [19] or idiopathic pulmonary fibrosis [20]. Since the serum levels well correspond to the status of diseases, periostin has been reported as a possible serum biomarker that may aid in deciding on treatment for asthma or other allergic diseases [21]. Regarding BA, periostin has been reported as a possible serum marker of liver fibrosis that reflects disease progression [22]. However, its presence in tissues of BA patients has never been examined, especially around the extrahepatic bile ducts.

In this study, we focused on the immunoreaction at the hepatic hilar area, the primary damaged region in BA patients. We analyzed the contribution of IL13 and its downstream factor periostin to the inflammation and fibrogenesis around the bile ducts by histological and cellular approaches.

Materials And Methods

Ethics

Tissue samples and clinical data were obtained from 32 BA patients who received surgery in our institution from January 2008 to March 2020. All patients were informed of the study and consented to their inclusion. The analyses of this study were approved by the ethics committee of our institution.

Histological analyses

Tissues from the hepatic hilar area resected at surgery were immediately fixed in 10% formalin and embedded in paraffin. Continuous 4-μm-thick sections were stained immunohistochemically using each primary antibody: 1:400 of anti-CD45 antibody (ab10558; abcam, Cambridge, UK), 1:6000 of anti-α-SMA antibody (1395-1-AP; Proteintech, Rosemont, IL, USA), 1:400 of anti-Interleukin 13 antibody (#06-1090; Merck, Darmstadt, Germany), and 1:500 of anti-periostin antibody (sc-398631; Santa Cruz Biotechnology, Dallas, TX, USA). Immunohistochemistry (IHC) was performed as follows: after deparaffinization, antigen unmasking was performed in pH 6.0 citrate buffer after heating with a microwave for 10 minutes. After cooling, slides were placed in methanol with 0.3% H_2O_2 for 30 minutes and then incubated in blocking solution (Blocking One Hist; Nacalai Tesque, Kyoto, Japan) for 1 h. Then sections were incubated with each primary antibody overnight in 4°C. Following phosphate-buffered saline (PBS) washing, sections were incubated for 30 minutes at room temperature with each appropriate secondary antibody

(Polyclonal Rabbit Anti-Human IgG/HRP, #P0214; Dako Cytomation, Glostrup, Denmark; and Goat Anti-Mouse IgG H&L [HRP], ab10558; abcam). Finally, sections were incubated for 5 to 10 minutes with Liquid DAB + Substrate (K3467; Dako), and cell nuclei were counterstained with hematoxylin. Stained sections were observed with a microscope, and images were captured and measured. Numbers of bile ducts were counted for each section, and immunological staining around bile ducts within 100 μm was evaluated.

Fibroblast culture from a BA patient

Small fragments of tissues were obtained from the hepatic hilar area of a BA patient at surgery. The tissues were dissected to further smaller pieces and incubated in DMEM low-glucose medium (Nacalai Tesque) containing 5% fetal bovine serum (FBS) (BioWest, Nuaillé, France) and Penicillin/Streptomycin (Nacalai Tesque). After cells had adhered to the culture dish and spread, they were passaged and used for experiments.

Immunofluorescence (IF)

IF was performed to confirm that the cultured cells were active fibroblasts by staining with α-SMA. Cells were fixed for 15 min with 4% paraformaldehyde and permeabilized for 1h with 0.3% Triton-X and 10% FBS in PBS. Cells were incubated overnight at 4°C in primary antibody solution containing 1:200 of anti-α-SMA antibody (1395-1-AP; Proteintech). Following PBS washes, cells were incubated for 30 minutes at room temperature in PBS containing 1:400 of secondary antibody labeled with Alexa Fluor 546 (Goat anti-Rabbit IgG(H + L); Thermo Fisher Scientific, Hudson, NH, USA). Finally, cells were encapsulated with DAPI for nuclear staining. Cells were observed by a fluorescence microscope.

Quantitative real-time polymerase chain reaction (qPCR)

Cultured fibroblasts were stimulated with Recombinant Human IL-13 (Pepro Tech, Cranbury, NJ, USA) at 1, 10, and 100 ng/ml for 72 h, and total RNA was extracted using a FastGeen RNA Basic Kit (NIPPON Genetics, Tokyo, Japan) following the manufacturer's protocol. cDNA was synthesized using PrimeScript RT Master MIX (TaKaRa Bio, Shiga, Japan). Real-time qPCR was performed by StepOnePlus (Thermo Fisher Scientific) using THUNDERBIRD SYBR qPCR Mix (TOYOBO, Osaka, Japan). Periostin gene expression was measured and normalized by Glyceraldehyde-3-Phosphate Dehydrogenase (GAPDH). Primers were manufactured by Thermo Fisher Scientific. The primer sequences were as follows (F for forward, R for reverse): Periostin: F: *CAGCAAACCACCTTCACGGATC*, R: *TTAAGGAGGCGCTGAACCATGC*, GAPDH: F: *GTCTCCTCTGACTTCAACAGCG*, R: ACCACCCTGTTGCTGTAGCCAA. Data were analyzed by the $\Delta\Delta C_T$ method, and the values were calculated as relative values to the non-treated control sample.

Western blotting (WB)

Fibroblasts were cultured with 100 ng/ml of recombinant Human IL-13 (Pepro Tech) for 96 h, and then total protein was obtained using RIPA buffer (08714; Nacalai Tesque). Each 10 μg of protein sample was reduced, and sodium dodecyl sulfate-polyacrylamide gel electrophoresis (SDS-PAGE) was performed using a Bio-Rad system. After transferring to a PVDF Membrane, (#1620174; Bio-Rad Laboratories, Hercules, CA), membranes were blocked in Blocking One (03953-95; Nacalai Tesque) for 1 h. Membranes

were incubated with 1:100 of anti-periostin antibody (sc-398631; Santa Cruz Biotechnology) and 1:1000 of anti-rabbit beta-actin antibody (#4967; Cell Signaling Technology, MA, USA). Following TBS-T washing, membranes were incubated for 1 h at room temperature with the appropriate secondary antibody (1:500 Mouse IgG Horseradish Peroxidase-conjugated Antibody, HAF007; R&D Systems, Minneapolis, MN, USA; and 1:1000 Rabbit IgG Horseradish Peroxidase-conjugated Antibody, HAF008; R&D Systems). Proteins were visualized using an enhanced chemiluminescence kit (ECL Select Western Blotting Detection Reagent; Cytiva, Tokyo, Japan) and ImageQuant LAS 500 (Cytiva).

Statistical analyses

Categorical data were compared using the chi-squared test (with Yates' correction when appropriate). All statistical analyses were performed using the StatMate software program (Version 5 for Win&Mac Hybrid; Atms, Chiba, Japan).

Results

Histological analyses of tissues resected from the hepatic hilar area of BA patients

Figure 1A total of 50 samples (right side: 23 samples, left side: 19 samples, unknown region: 8 samples) from 32 BA patients were analyzed. The total number of bile ducts counted in the tissues was 745. We distinguished the bile ducts as large and micro ducts according to the diameter (≥150 or <150 μm, respectively). This was because the large ducts show more damaged epithelium and seemed to be original ducts, whereas micro ducts were round and rather well-preserved, presumed to be newly generated ducts or peribiliary glands (Figure 1a-d). The total number of large ducts was 150, and the total number of micro ducts was 595.

To analyze the inflammatory cell infiltration around the bile ducts, immunostaining for CD45 was performed. CD45 was stained as a marker of leucocytes in small round cells forming clusters around the bile ducts (Figure 1a). CD45 was positive around 659 of the 745 bile ducts (88.5%) and was particularly remarkable around the large ducts (140 of 150 ducts, 93.3%). IL13 staining was also performed, and the pattern was compared with the staining of CD45. IL13 staining was found among infiltrating cells as well as in the bile duct epithelium (Figure 1c). IL13 was positive around 135 large ducts (90%) and 558 micro ducts (93%), with no marked preference of staining noted among duct sizes (Table 1). Regarding large ducts, IL13 was positive in 92.1% (P=0.006) of CD45-positive ducts (Table 2).

Table 1
Numbers and ratios of bile ducts stained with each marker

	Large + micro	(%)	Large ducts (≥ 150 μm)	(%)	Micro ducts (< 150 μm)	(%)	P value
Total	745		150		595		
CD45-positive	659	(88.5)	140	(93.3)	519	(87.2)	0.036
IL13-positive	693	(93)	135	(90)	558	(93.8)	0.104
α-SMA-positive	389	(52.2)	110	(73.3)	279	(46.9)	< 0.001
Periostin-positive	520	(69.8)	121	(80.7)	399	(67.1)	0.001

Table 2
Colocalization of IL13 and CD45 around large bile ducts

	IL13-positive	IL13-negative	Total
CD45-positive	129	11	140
CD45-negative	6	4	10
Total	135	15	150
Chi-square test (Yates correction): p-value = 0.006 φ = 0.22			

We also performed immunostaining for α-SMA and periostin to analyze the active fibrosis around bile ducts. Both markers were stained more around large ducts than around micro ducts (Figure 1b,1d). α-SMA was positive in 73.3% (110 of 150) of large ducts and 46.9% (279 of 595) of micro ducts (p<0.001). Periostin was positive in 80.7% (121 of 150) of large ducts and 67.1% (399 of 595) of micro ducts (Table 1). Regarding large ducts, periostin positivity was noted in 90.9% (p<0.001) of α-SMA-positive ducts (Table 3).

Table 3
Colocalization of α-SMA and periostin around large bile ducts

	Periostin-positive	Perisotin-negative	Total
α-SMA-positive	100	10	110
α-SMA-negative	21	19	40
Total	121	29	150
Chi-square test: p-value < 0.001 φ = 0.43; odds ratio = 9.05			

Since periostin is known to be induced from fibroblasts by IL13, we analyzed the correlation of periostin, α-SMA and IL13 (Table 4). Periostin staining was significantly dominant around ducts with both α-SMA and IL13 staining (90.3%, $p<0.001$).

Table 4
Colocalization of IL13/α-SMA and periostin in large bile ducts

	Periostin-positive	Perisotin-negative	Total
IL13positive and α-SMA positive	93	10	103
IL13 negative or α-SMA negative	28	19	47
Total	121	29	150
Chi-square test: p-value < 0.001 φ = 0.36; odds ratio = 6.31			

In summary, IL13 staining was found around large bile ducts with inflammatory cell infiltration as well as in the epithelium of micro bile ducts. Fibrotic markers α-SMA and periostin were significantly positive around large bile ducts, corresponding to IL13-positive regions.

Induction of periostin by IL13 stimulation in fibroblasts derived from BA tissue

Figure 2

The cultured cells, originally obtained from the hepatic hilar area tissues of a BA patient, were spindle-shaped and α-SMA positive by immunofluorescence and confirmed to be active fibroblasts (Figure 2a). Both periostin mRNA expression and protein production from cells by recombinant IL13 stimulation were analyzed using qPCR and WB. Periostin mRNA expression was dose-dependently elevated by 72 h of IL13 stimulation, and the value with 100 ng/ml stimulation was about 4-fold that in untreated cells (Figure 2b). The protein analysis showed the different forms of periostin, including a 90-kDa secretory glycoprotein and 84/74-kDa isoform. Bands of these forms were stronger in a sample of cells with IL13 treatment than in untreated cells on WB (Figure 2c).

In summary, we cultured fibroblasts obtained from the hepatic portal area of BA patients. Periostin production was induced by stimulation with recombinant IL13, and the upregulation was confirmed for both mRNA and protein.

Discussion

In this study, we found that IL13 was located at the region of inflammatory cell infiltration around the bile ducts of BA patients according to histological analyses of tissues from the hilar area of the liver. Furthermore, a downstream factor of IL13, periostin, was found around the remains of large bile ducts matched to the location of IL13 and α-SMA, at the site of active fibroblasts. The periostin production by

IL13 was also confirmed by *in vitro* analyses with cultured fibroblasts from BA patients. These results show the actual process of fibrogenesis at the extrahepatic bile ducts of BA: the immunocytes around the bile ducts produce IL13, which has marked effects on fibroblasts and the production of periostin.

While several immunological studies have reported type 1 immune responses in BA patients [12, 13], type 2 responses have been rarely reported. However, Li et al. reported that IL33, a member of the IL1 family of cytokines that is known to activate the type 2 immune response, was released from the epithelium of bile ducts by cytotoxic injury, causing cholangiocyte proliferation and rapid enlargement of the extrahepatic bile ducts in mice. They further showed that this response was mediated by IL-13 released from increased type 2 innate lymphoid cells (ILC2s) induced by IL33 stimulation [17]. Their findings correspond well to ours in tissues of BA patients. IL13 reportedly plays roles in cell proliferation in allergic diseases, such as asthma [23]. In our analyses, IL13 was detected not only among fibroblasts but also at the epithelium of micro bile ducts, which were found in the fibrotic remnants from the hepatic hilar area. It is suggested that IL13 plays roles in not only the fibrogenesis but also the proliferation of cholangiocytes and production of micro bile ducts.

Periostin has been well studied for its involvement in allergic inflammation and fibrosis disease, and it is known to be expressed in epithelium and fibroblasts [19, 20]. Mitamura et al. reported the involvement of oxidative stress in the expression of periostin, which is mediated by TGF-β1 and IL-13 in normal human dermal fibroblasts [24]. The correlation between liver fibrosis and periostin has also been reported. A previous report revealed that periostin expression was significantly upregulated in a mouse model of chronic liver fibrosis induced by carbon tetrachloride and bile duct ligation [25]. Regarding BA, periostin levels in post-KPE serum samples have been assessed, and the association with ultrasonography hepatic fibrosis scores has been evaluated [22]. Our findings also suggest the association of periostin expression with active fibrogenesis around bile ducts at KPE. As a biomarker, periostin is detected in very high concentrations in serum and is easily measured by an immunoassay. Recently, many assay methods for periostin detection have been developed [21, 26]. Serum periostin levels may thus be useful as a biomarker in BA before primary surgery. Further investigations and follow-up of the periostin expression, including serum, in BA patients are thus needed.

In conclusion, we found that IL13 was associated with cholangiocyte proliferation and induced periostin expression by fibroblasts, playing a vital role in the pathogenesis of fibrogenesis around the extrahepatic bile duct in BA. In the future, it will be necessary to accumulate data and conduct more detailed investigations into the involvement of periostin and IL13 in pathological conditions.

References

1. Chandra RS, Altman RP (1978) Ductal remnants in extrahepatic biliary atresia A histopathologic study with clinical correlation. J Pediatr 93:196–200. https://doi.org/10.1016/s0022-3476(78)80495-8

2. Tan CEL, Davenport M, Driver M, Howard ER (1994) Does the morphology of the extrahepatic biliary remnants in biliary atresia influence survival? A review of 205 cases. J Pediatr Surg 29:1459–1464. https://doi.org/10.1016/0022-3468(94)90144-9
3. Altmam RP, Lilly JR, Greenfeld J, Weinberg A, van Leeuwem K, Flanigan L (1997) A multivariable risk factor analysis of the portoenterostomy (Kasai) procedure for biliary atresia: twenty-five years of experience from two centers. Ann Surg 226:348–353. https://doi.org/10.1097/00000658-199709000-00014
4. Wildhaber BE, Coran AG, Drongowski RA, Hirschl RB, Geiger JD, Lelli JL, Teitelbaum DH (2003) The Kasai portoenterostomy for biliary atresia: a review of a 27-year experience with 81 patients. J Pediatr Surg 38:1480–1485. https://doi.org/10.1016/s0022-3468(03)00499-8
5. Mirza Q, Kvist N, Petersen BL (2009) Histologic features of the portal plate in extrahepatic biliary atresia and their impact on prognosis-a Danish study. J Pediatr Surg 44:1344–1348. https://doi.org/0.1016/j.jpedsurg.2008.11.054
6. Nguyen AP, Pham YHT, Vu GH, Nguyen MH, Hoang TN, Holterman A (2021) Biliary atresia liver histopathological determinants of early post-Kasai outcome. J Pediatr Surg 56: 1169–1173. https://doi.org/10.1016/j.jpedsurg.2021.03.039
7. Lawrence D, Howard ER, Tzannatos C, Mowat AP (1981) Hepatic portoenterostomy for biliary atresia. A comparative study of histology and prognosis after surgery. Arch Dis Child 56:460–463. https://doi.org/10.1136/adc.56.6.460
8. Langenburg SE, Poulik J, Goretsky M, Klein AA, Klein MD (2000) J Pediatr Surg 35:1006–1007. https://doi.org/10.1053/jpsu.2000.6954
9. Mannon P, Reinisch W (2012) Interleukin 13 and its role in gut defence and inflammation. Gut 61:1765–1773. https://doi.org/10.1136/gutjnl-2012-303461
10. Gieseck RL3rd, Wilson MS, Wynn TA (2018) Type 2 immunity in tissue repair and fibrosis. Nat Rev Immunol 18:62–76. https://doi.org/10.1038/nri.2017.90
11. Mao YM, Zhao CN, Leng J, Leng RX, Ye DQ, Zheng SG, Pan HF (2019) Interleukin-13: A promising therapeutic target for autoimmune disease. Cytokine Growth Factor Rev 45:9–23. https://doi.org/10.1016/j.cytogfr.2018.12.001
12. Mack CL, Tucker RM, Sokol RJ, Karrer FM, Kotzin BL, Whitington PF, Miller SD (2004) Biliary Atresia Is Associated with CD4 + Th1 Cell–Mediated Portal Tract Inflammation. Pediatr Res 56:79–87. https://doi.org/10.1203/01.pdr.0000130480.51066.fb
13. Shivakumar P, Mourya R, Bezerra JA (2014) Perforin and granzymes work in synergy to mediate cholangiocyte injury in experimental biliary atresia. J Hepatol 60:370–376. https://doi.org/10.1016/j.jhep.2013.09.021
14. Liu J, Yang Y, Zheng C, Chen G, Shen Z, Zheng S, Dong R (2019) Correlation of Interleukin-33/ST2 Receptor and Liver Fibrosis Progression in Biliary Atresia Patients. Front Pediatr 7:403. https://doi.org/10.3389/fped.2019.00403

15. Adawy N, El-Araby H, Allam A, Elshenawy S, Khedr M, Ibrahim Y, Zakaria HM (2018) Serum level of interleukin-13 receptor alpha 2 in infants with biliary atresia - is it of value? Clin Exp Hepatol 4:91–96. https://doi.org/10.5114/ceh.2018.75958
16. Li J, Bessho K, Shivakumar P, Mourya R, Mohanty SK, Dos Santos JL, Miura IK, Porta G, Bezerra JA (2011) Th2 signals induce epithelial injury in mice and are compatible with the biliary atresia phenotype. J Clin Invest 121:4244–4256. https://doi.org/10.1172/JCI57728
17. Li J, Razumilava N, Gores GJ, Walters S, Mizuochi T, Mourya R, Bessho K, Wang YH, Glaser SS, Shivakumar P, Bezerra JA (2014) Biliary repair and carcinogenesis are mediated by IL-33-dependent cholangiocyte proliferation. J Clin Invest 124:3241–3251. https://doi.org/10.1172/JCI73742
18. Izuhara K, Nunomura S, Nanri Y, Ogawa M, Ono J, Mitamura Y, Yoshihara T (2017) Periostin in inflammation and allergy. Cell Mol Life Sci 74:4293–4303. https://doi.org/10.1007/s00018-017-2648-0
19. Takayama G, Arima K, Kanaji T, Toda S, Tanaka H, Shoji S, McKenzie AN, Nagai H, Hotokebuchi T, Izuhara K (2006) Periostin: a novel component of subepithelial fibrosis of bronchial asthma downstream of IL-4 and IL-13 signals. J Allergy Clin Immunol 118:98–104. https://doi.org/10.1016/j.jaci.2006.02.046
20. Okamoto M, Hoshino T, Kitasato Y, Sakazaki Y, Kawayama T, Fujimoto K, Ohshima K, Shiraishi H, Uchida M, Ono J, Ohta S, Kato S, Izuhara K, Aizawa H (2011) Periostin, a matrix protein, is a novel biomarker for idiopathic interstitial pneumonias. Eur Respir J 37:1119–1127. https://doi.org/10.1183/09031936.00059810
21. Izuhara K, Ohta S, Ono J (2016) Using Periostin as a Biomarker in the Treatment of Asthma. Allergy Asthma Immunol Res 8:491–498. https://doi.org/10.4168/aair.2016.8.6.491
22. Honsawek S, Udomsinprasert W, Vejchapipat P, Chongsrisawat V, Phavichitr N, Poovorawan Y (2015) Elevated serum periostin is associated with liver stiffness and clinical outcome in biliary atresia. Biomarkers 20:157–161. https://doi.org/10.3109/1354750X.2015.1045032
23. Marone G, Granata F, Pucino V, Pecoraro A, Heffler E, Loffredo S, Scadding GW, Varricchi, G (2019) The Intriguing Role of Interleukin 13 in the Pathophysiology of Asthma. Front Pharmacol 10:1387. https://doi.org/10.3389/fphar.2019.01387
24. Mitamura Y, Murai M, Mitoma C, Furue M (2018) NRF2 Activation Inhibits Both TGF-beta1- and IL-13-Mediated Periostin Expression in Fibroblasts: Benefit of Cinnamaldehyde for Antifibrotic Treatment. Oxid Med Cell Longev 2018:1–10. https://doi.org/10.1155/2018/2475047
25. Huang Y, Liu W, Xiao H, Maitikabili A, Lin Q, Wu T, Huang Z, Liu F, Luo Q, Ouyang G (2015) Matricellular protein periostin contributes to hepatic inflammation and fibrosis. Am J Pathol 185:786–797. https://doi.org/10.1016/j.ajpath.2014.11.002
26. Ono J, Takai M, Kamei A, Azuma Y, Izuhara K (2021) Pathological Roles and Clinical Usefulness of Periostin in Type 2 Inflammation and Pulmonary Fibrosis. Biomolecules 11:1084. https://doi.org/10.3390/biom11081084

Figures

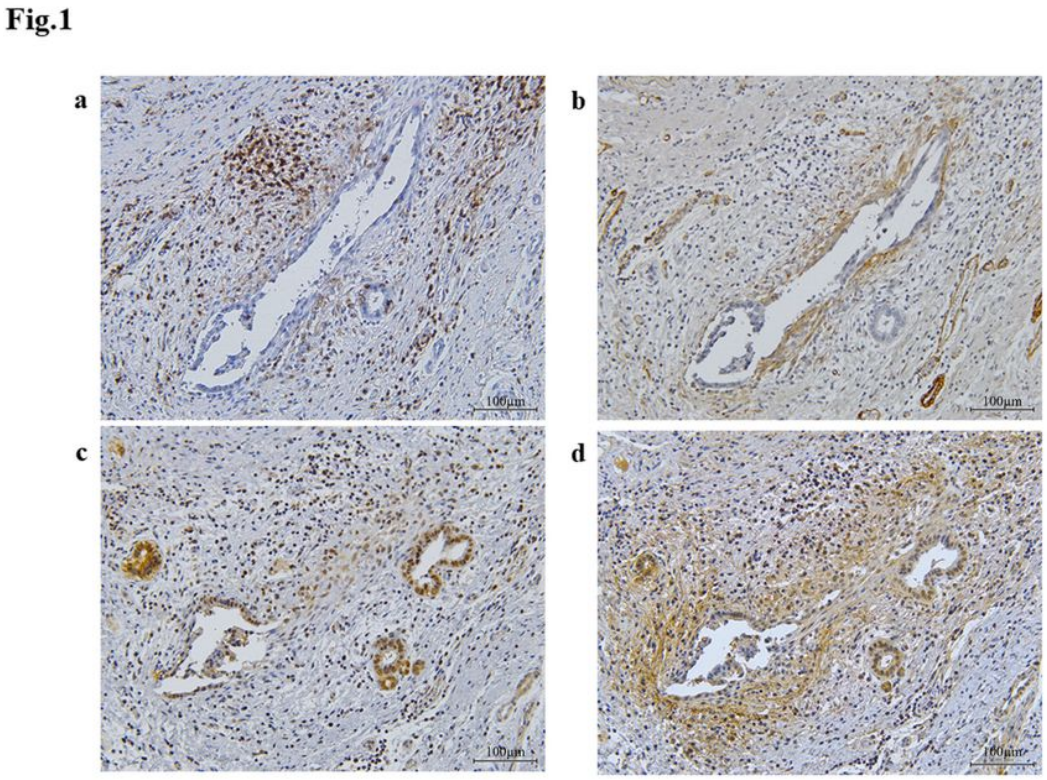

Figure 1

Examples of the bile duct sizes and immunohistochemical staining patterns in continuous sections of tissue. A large bile duct (≧150 μm) is located in the center, and micro ducts (<150 μm) surround the large duct. a: CD45, b: α-SMA, c: IL13, and d: Periostin staining.

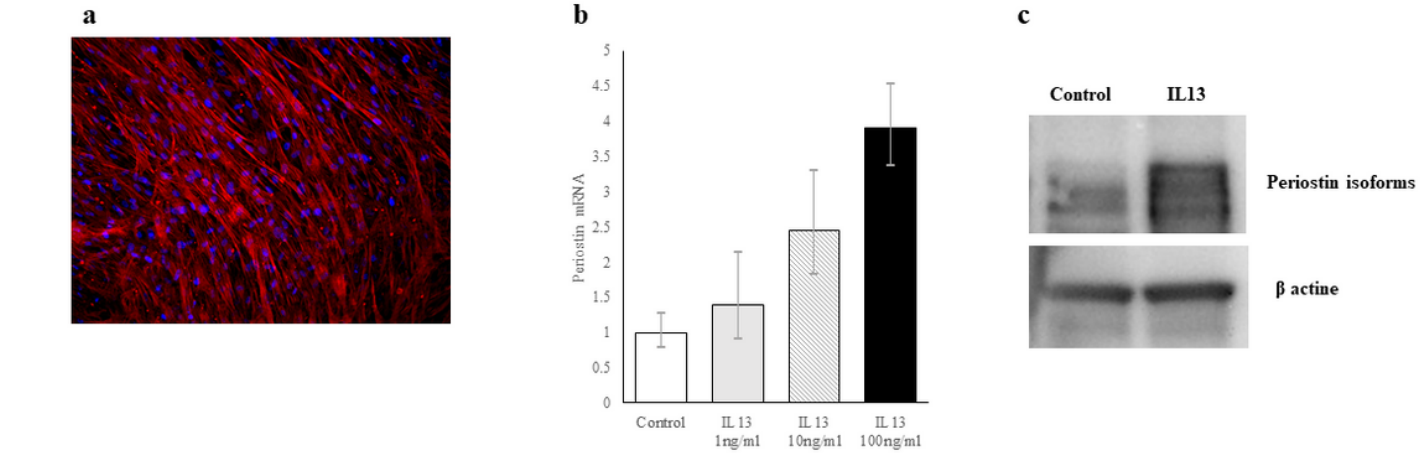

Figure 2

Periostin production analyses using cultured fibroblasts derived from a BA patient. Fragments of tissues were resected from the hepatic hilar area at surgery and cultured, and proliferated cells were confirmed to be fibroblasts by immunofluorescent staining of α-SMA (a). b: qPCR findings for periostin expression in fibroblasts with or without IL13 stimulation. Periostin expression was upregulated dose-dependently by 72 h of IL13 stimulation. c: Western blotting targeting periostin protein. Fibroblasts were cultured with 100 ng/ml of IL13 for 96 h, and then protein production was compared with that in an untreated control. Periostin protein was elevated by IL13 stimulation.